Origins of Radial and Axial Inhomogeneity of Magnetic Performance in Cylindrical Nd-Fe-B Magnet Prepared by Hot Deformation

Wen-Zong Yin[1,2], Ren-Jie Chen[1,2], Xu Tang[1,2], Xin Tang[1,2], Don Lee[1,2], and Aru Yan[1,2]

[1]Key Laboratory of Magnetic Materials and Devices, Ningbo Institute of Material Technology and Engineering, Chinese Academy of Sciences, Zhenhai, Ningbo, Zhejiang 315201, P. R. China
[2]Zhejiang Province Key Laboratory of Magnetic Materials and Application Technology, Ningbo Institute of Material Technology and Engineering, Chinese Academy of Sciences, Zhenhai, Ningbo, Zhejiang 31520, P. R. China

Cylindrical Nd-Fe-B magnets with different height reductions were prepared by hot deformation method. The inhomogeneity of the magnetic performance along the radial direction was revealed with a closed circuit B-H apparatus while that along the axial direction was shown with a vibrating sample magnetometer. The microstructure examined with scanning electron microscopy suggests that orientation variation and grain coarsening of $Nd_2Fe_{14}B$ platelets cooperate to result in the deterioration of remanence along radial direction from center to edge. X-ray diffractometry was carried out over the end surfaces and axially across the middle cross-section of the cylindrical magnet, showing the important role of texture in determination of remanence along the axial direction. Further investigations on an intermediate hot-deformed magnets reveal the unevenness of deformation degree in the axial direction during hot deformation, which accounts for the axial variation of texture and consequent remanence.

Index Terms—Hot deformation, inhomogeneity, Nd-Fe-B, texture.

I. Introduction

HOT DEFORMED (HD) Nd-Fe-B magnets exhibit good magnetic performance [1], [2], corrosion resistance [3], [4] and thermal stability [5]. Therefore, increased attention has been drawn to them in both basic and application research fields [6]–[8], focusing mainly on ring-shaped and cylindrical HD magnets [9]. Today, a ring-shaped HD magnet could be easily prepared by a special hot deformation technique called backward extrusion method. Detailed investigation revealed that its magnetic performance was inhomogeneous along both axial and radial directions [10]. In the axial direction, remanence (B_r) increased monotonically from the top to bottom part of the ring-shaped HD magnet while coercivity (H_{ci}) decreased simultaneously [11], [12]. In the radial direction, a ring-shaped HD magnet displayed an approximate linear enhancement of B_r from the outer to inner surface [6], [13]. For the cylindrical HD magnet, Guruswamy *et al.* presented a theoretical investigation on the inhomogeneity of deformation via simulation method using a finite-element-based software called "ANTARES" [14]. However, systematic experimental investigations were not reported on the homogeneities of the magnetic performance in cylindrical HD magnets along either the radial or axial direction.

For metals and alloys with a cylindrical shape, it was reported that material flow during plastic deformation is uneven in the axial direction due to the existence of friction at both end surfaces contacted with punches [15]. Therefore, material flow at the axially middle cross-section is easier than that at end surfaces. As a ternary alloy, Nd-Fe-B could be deformed from a
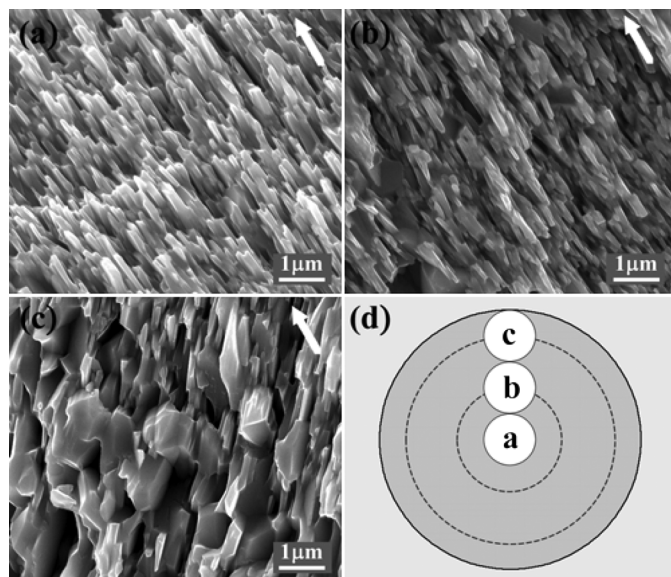

Fig. 1. (a), (b) and (c): SEM images of the type-I samples cut off from different radial positions of HDM-3. (d) Schematic illustration on the positions of type-I samples in HDM-3 (top view). White arrows represent radial direction.

thin cylinder into a fat one at 650 °C–850 °C [16], [17]. The unevenness of material flow in a Nd-Fe-B magnet during this deformation was merely mentioned in [18]. No further experimental investigation was carried out to the best of our knowledge.

In this paper, the inhomogeneities of magnetic performance were demonstrated both in the axial and radial directions. The origins of the inhomogeneities were revealed in terms of microstructures and the material flow during deformation.

II. Experimental Work

Melt-spun powder (MQU-F) was purchased from Magnequench International, Inc., and used as raw material without any treatment. The powder was firstly compacted into a green
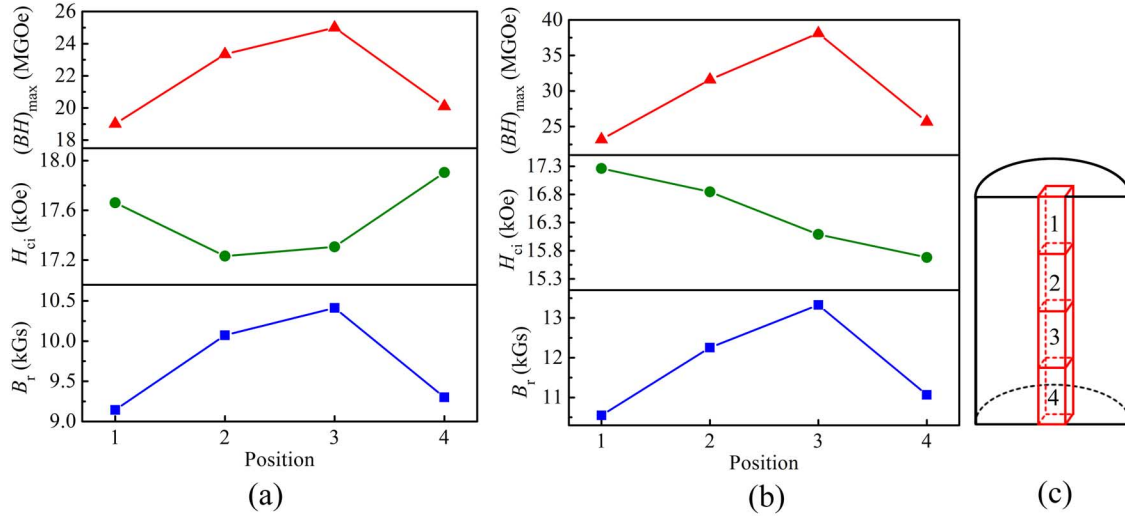
Fig. 2. Variations of the B_r, H_{ci} and $(BH)_{max}$ of type-II samples over axial positions for (a) HDM-1 and (b) HDM-2. (c) Schematic illustration on the positions of type-II samples.

Position	B_r (kGs)	H_{ci} (kOe)	$(BH)_{max}$ (MGOe)
a	13.28	14.72	43.3
b	13.15	15.56	42.9
c	12.75	15.08	39.9

body (Φ13 mm $*$ 24 mm) under vacuum at 943 K and a pressure of 200 MPa. Then the green body was deformed in a tungsten carbide (WC) die at 1113 K under argon atmosphere. The illustrations of the compaction and deformation were presented in [19]. HD magnets with the height reduction (HR) of 28.1%, 53.2% and 70% were prepared using WC dies with the diameters of 15.3 mm, 19.0 mm and 24 mm. They were denoted as HDM-1, HDM-2 and HDM-3, respectively. Cylindrical samples (type-I) with the dimensions of Φ6 mm $*$ 6 mm were cut off from the HD magnet with the HR of 70%, as shown in Fig. 1. The magnetic performance of type-I samples was measured along the easy direction, which is parallel to the pressing direction, with a closed circuit B-H apparatus at room temperature. The samples were premagnetized with a dc pulse field of 29 kOe. Rectangular samples (type-II) with the dimensions of 1.5 mm $*$ 1.5 mm $*$ 2 mm were cut off from the HD magnet with the HR of 28.1% and 53.2%, as shown in Fig. 2. Their magnetic performance was measured along the easy axis through a Lakeshore 7400 vibrating sample magnetometer (VSM) in an applied field up to 23 kOe without demagnetization field correction. The phase composition was identified using an X-ray diffractometer (XRD, Bruker AXS D8 Advance) with Cu Kα radiation. Microstructures of samples were examined on a field emission scanning electron microscope (FE-SEM, Hitachi S-4800).

III. RESULTS AND DISCUSSION

Table I presents the B_r, H_{ci} and maximum energy product ($(BH)_{max}$) of the type-I samples cut from different positions of HDM-3 along radial direction. Both B_r and $(BH)_{max}$ decrease

monotonically from positions a to c. The maximum difference in B_r and $(BH)_{max}$ is about 0.53 kGs and 3.4 MGOe. But H_{ci} firstly increases from 14.72 kOe at position a to 15.56 kOe at position b and then decreases to 15.08 kOe at position c. These results reveal that the magnetic performance of cylindrical HD magnet is inhomogeneous along the radial direction. B_r and $(BH)_{max}$ at the center are higher than those at the edge.

To reveal the reasons for the declined B_r along the radial direction, microstructures were examined with SEM over the cross sections of the type-I samples. The results are shown in Fig. 1. At position a, $Nd_2Fe_{14}B$ grains exhibit platelet shape and good alignment [Fig. 1(a)]. The thickness of these grains is about 100-150 nm. At position b, some coarse grains appear while most remain platelet [Fig. 1(b)]. At position c [Fig. 1(c)], the number of coarse grains increased remarkably. Meanwhile, it should be noted that the alignment orientation of $Nd_2Fe_{14}B$ grains at position c is not parallel with that at position a and b. Grain coarsening was reported to be an important reason for the decline of crystal alignment in the HD magnet [10]. But the above results further reveal the key role of orientation difference in the deterioration of crystal alignment and consequent B_r.

Fig. 2 shows the magnetic performance of the type-II samples cut from different axial positions of HDM-1 and HDM-2. Both of them show inhomogeneous magnetic performance in the axial direction. Concretely, B_r and $(BH)_{max}$ at positions 2 and 3 are much higher than those at positions 1 and 4. When HR is 28.1% [Fig. 2(a)], the highest B_r and $(BH)_{max}$ are 10.4 kGs and 25.0 MGOe. The corresponding samples are located at position 3. The lowest B_r and $(BH)_{max}$ are measured to be 9.1 kGs and 19.0 MGOe on the samples at position 1. The difference between them in B_r and $(BH)_{max}$ is 1.3 kGs and 6.0 MGOe, respectively. When HR is 53.2% [Fig. 2(b)], the highest B_r and $(BH)_{max}$ increase to 13.0 kGs and 38.1 MGOe at position 3 and the lowest to 10.2 kGs and 23.2 MGOe at position 1. The difference between them in B_r and $(BH)_{max}$ is enlarged to 2.8 kGs and 14.9 MGOe, respectively. The above results reveal that the axially middle part of the cylindrical HD magnet exhibits higher B_r and $(BH)_{max}$ than both end parts. On the other hand, H_{ci}
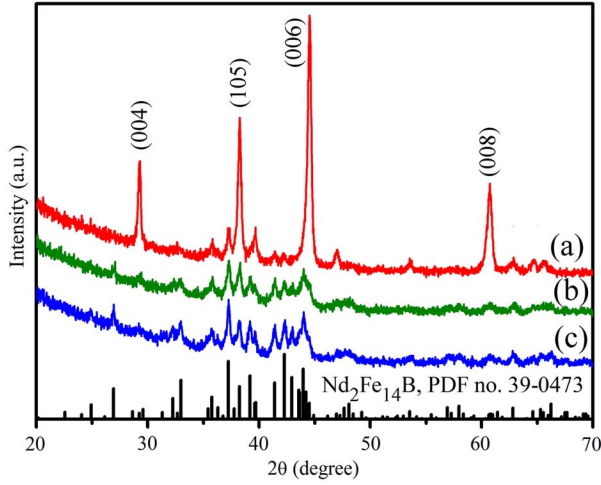
Fig. 3. XRD patterns over (a) interface between samples 2 and 3 in Fig. 2(c), (b) top surface, and (c) bottom surface of the HDM-2.
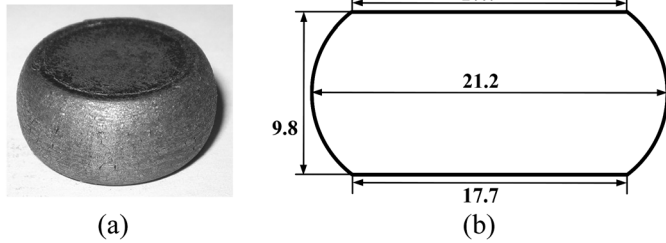

Fig. 4. (a) Photograph of the intermediate HD magnet with the HR of 53.2%. (b) Dimensions of the intermediate HD magnet (unit: mm).

displays an opposite variation over axial position when HR is 28.1%. The samples at positions 2 and 3 have significantly lower H_{ci} than those at positions 1 and 4. But when HR is 53.2%, H_{ci} displays a monotonic decrease from 17.3 kOe at position 1 to 15.7 kOe at position 4. The reason for this phenomenon needs further investigation.

As B_r of the HD magnet is determined by texture to a great extent, the texture of HDM-3 was evaluated with XRD over two end surfaces and the interface between sample 2 and 3. The results are shown in Fig. 3. For the interface between samples 2 and 3, the intensity of (004), (006) and (008) crystal planes is much higher than the others, indicating good texture at this interface. Both end surfaces, however, exhibit little texture. The big difference in texture along the axial direction accounts for the axial inhomogeneity of the magnetic performance in the HD magnet.

To reveal the origins of texture difference along axial direction, an intermediate HD magnet with HR of 53.2% was prepared using a WC die with the diameter of 24 mm (maximum HR is 70%). Fig. 4 represents the photograph of this intermediate HD magnet and its dimensions. The intermediate magnet appears like a barrel whose axially middle part bulges out [Fig. 4(a)]. The diameters along its axial direction are different [Fig. 4(b)]. The diameter of the two end surfaces is 17.7 mm, which is the minimum. The maximum diameter is 21.2 mm, located at the middle of the magnet in the axial direction. The thickness of the intermediate magnet is 9.8 mm.

TABLE II
MAGNETIC PERFORMANCE OF SAMPLES (1.5 mm * 1.5 mm * 2 mm) CUT FROM DIFFERENT REGIONS OF INTERMEDIATE HD MAGNET AS ILLUSTRATED IN FIG. 5

Samples	B_r (kGs)	H_{ci} (kOe)	$(BH)_{max}$ (MGOe)
IM-1	10.92	17.46	27.17
IM-2	13.56	15.71	43.55
IM-3	9.95	18.26	23.61

Fig. 5. Schematic illustration on the positions of IM series samples cut from intermediate HD magnet with the HR of 53.2%.

This barrel-like shape should result from the unevenness in the plastic deformation of Nd-Fe-B alloy due to the existence of friction at both end surfaces contacted with punches [15].

Deformation degree (η) could be evaluated in two ways. One is by height reduction (HR) as follows [20]:

$$\eta = HR = \frac{h_0 - h}{h_0} \tag{1}$$

where h_0 is the height of green body before hot deformation, and h is the height of HD magnet. Alternatively, deformation degree could also be calculated from the cross-section area of cylindrical HD magnet with the following:

$$\eta = \frac{S - S_0}{S} = 1 - \left(\frac{d_0}{d}\right)^2 \tag{2}$$

where d_0 and d are the diameters of cylindrical magnets before and after hot deformation. S_0 and S are the cross-section areas of cylindrical magnets before and after hot deformation. Due to the constant volume of the magnet before and after deformation, the above two methods are equivalent for the cylindrical HD magnet. But when it comes to the barrel-shaped intermediate HD magnet, only (2) is appropriate for evaluating deformation degree. Equation (1) just presents an average deformation degree of the whole magnet. For the as-prepared intermediate magnet, η is estimated to be 53.2% from $h(9.8$ mm) and $h_0(21$ mm) by (1). Nonetheless, η is calculated to be 44.4% by (2) from the minimum diameter (17.7 mm) at the end surface of the intermediate magnet and 61.2% from the maximum (21.2 mm) at the middle cross section. Such a difference in η plays an important role in the variation of texture and consequent B_r along the axial direction.

Table II lists the magnetic performance of IM series samples (1.5 mm * 1.5 mm * 2 mm) cut from different axial regions of the intermediate HD magnet (Fig. 5). The B_r of sample IM-2 (13.56 kGs) is much higher than that of IM-1 (10.92 kGs) and IM-3 (9.95 kGs). This is consistent with the variations of both B_r in Fig. 2 and texture in Fig. 3, confirming the key role of η in the variation of B_r along axial direction.

IV. CONCLUSION

Cylindrical HD magnet exhibits inhomogeous magnetic performance in both radial and axial directions. Along the radial direction, B_r at position a is higher than that at position c due to the orientation variation and grain coarsening at the edge. In the axial direction, the HD magnet shows a higher B_r at the axially middle region than that near both end surfaces, which is ascribed to the variation of texture at different axial positions. Furthermore, such variation in texture results from the unevenness of deformation degree due to the existence of friction at both end surfaces contacted with punches.

REFERENCES

[1] M. Leonowicz, D. Derewnicka, M. Wozniak, and H. A. Davies, "Processing of high-performance anisotropic permanent magnets by die-upset forging," *J. Mater. Process. Technol.*, vol. 153, pp. 860–867, 2004.

[2] S. Liu, D. Lee, M. Huang, and A. Higgins, "Research and development of bulk anisotropic nanograin composite rare earth permanent magnets," *J. Iron. Steel. Res. Int.*, vol. 13, pp. 123–135, 2006.

[3] B. M. Ma, D. Lee, B. Smith, S. Gaiffi, B. Owens, H. Bie, and G. W. Warren, "Comparison of the corrosion behavior of die-upset and sintered NdFeB magnets," *IEEE Trans. Magn.*, vol. 37, no. 5, pp. 2477–2479, Oct. 2001.

[4] A. A. El-Moneim, O. Gutfleisch, A. Plotnikov, and A. Gebert, "Corrosion behaviour of hot-pressed and die-upset nanocrystalline NdFeB-based magnets," *J. Magn. Magn. Mater.*, vol. 248, pp. 121–133, 2002.

[5] N. Yoshikawa, Y. Kasai, T. Watanabe, S. Shibata, V. Panchanathan, and J. J. Croat, "Effect of additive elements on magnetic properties and irreversible loss of hot-worked Nd-Fe-Co-B magnets," *J. Appl. Phys.*, vol. 69, pp. 6049–6051, 1991.

[6] W. Grunberger, D. Hinz, A. Kirchner, K. H. Muller, and L. Schultz, "Hot deformation of nanocrystalline Nd-Fe-B alloys," *J. Alloy. Compd.*, vol. 257, pp. 293–301, 1997.

[7] K. Khlopkov, O. Gutfleisch, D. Hinz, K. H. Muller, and L. Schultz, "Evolution of interaction domains in textured fine-grained $Nd_2Fe_{14}B$ magnets," *J. Appl. Phys.*, vol. 102, p. 023912, 2007.

[8] D. Hinz, A. Kirchner, D. N. Brown, B. M. Ma, and O. Gutfleisch, "Near net shape production of radially oriented NdFeB ring magnets by backward extrusion," *J. Mater. Process. Technol.*, vol. 135, pp. 358–365, 2003.

[9] S. Sugimoto, "Current status and recent topics of rare-earth permanent magnets," *J. Phys. D: Appl. Phys.*, vol. 44, p. 064001, 2011.

[10] A. H. Li, W. Li, B. Lai, H. J. Wang, M. G. Zhu, and W. Pan, "Investigation on microstructure, texture, and magnetic properties of hot deformed Nd-Fe-B ring magnets," *J. Appl. Phys.*, vol. 107, p. 09A725, 2010.

[11] O. Gutfleisch, A. Kirchner, W. Grunberger, D. Hinz, R. Schafer, L. Schultz, and I. R. Harris, "Backward extruded NdFeB HDDR ring magnets," *J. Magn. Magn. Mater.*, vol. 183, pp. 359–364, 1998.

[12] H. T. Kim and Y. B. Kim, "Microstructure and magnetic properties of backward extruded NdFeB ring magnets by the CAPA process," *Phys. Status. Solidi. A*, vol. 201, pp. 1926–1929, 2004.

[13] W. Grunberger, D. Hinz, D. Schlafer, and L. Schultz, "Microstructure, texture, and magnetic properties of backward extruded NdFeB ring magnets," *J. Magn. Magn. Mater.*, vol. 157, pp. 41–42, 1996.

[14] S. Guruswamy, Y. R. Wang, and V. Panchanathan, "Plastic deformation modeling of die-upset process for magnequench NdFeB magnets," *J. Appl. Phys.*, vol. 83, pp. 6393–6395, 1998.

[15] V. Boljanovic, *Metal Shaping Processes: Casting and Molding, Particulate Processing, Deformation Processes, and Metal Removal*. New York, NY, USA: Industrial Press, 2009.

[16] Z. H. Hu, J. Li, L. H. Chu, and Y. Liu, "Effect of hot deformation temperature on the magnetic and mechanical properties of Nd-Fe-B magnets prepared by spark plasma sintering," *J. Magn. Magn. Mater.*, vol. 323, pp. 104–107, 2011.

[17] M. Lin, H. J. Wang, P. P. Yi, and A. R. Yan, "Effects of excessive grain growth on the magnetic and mechanical properties of hot-deformed NdFeB magnets," *J. Magn. Magn. Mater.*, vol. 322, pp. 2268–2271, 2010.

[18] L. Li and J. C. D. Graham, "Mechanism of texture formation by hot deformation in rapidly quenched FeNdB," *J. Appl. Phys.*, vol. 67, pp. 4756–4758, 1990.

[19] P. P. Yi, M. Lin, H. J. Wang, A. Yan, and D. Li, "Effect of hot-pressed progress on the magnetic properties of die-upset Nd-Fe-B magnets," *Rare Metal Mat. Eng.*, vol. 38, pp. 576–578, 2009.

[20] H. T. Kim, S. H. Cho, Y. B. Kim, K. S. Ryu, G. A. Kapustin, and H. S. Kim, "NdFeB thin anisotropic magnets obtained by hot working process," *J. Magn. Magn. Mater.*, vol. 272, pp. e1925–e1927, 2004.